Morphological Properties of Composite Solid Polymer Electrolytes Based on Polyethylene Oxide

ENRIQUE MORALES, JOSE LUIS ACOSTA

Instituto de Ciencia y Tecnología de Polímeros (C.S.I.C.), c/o Juan de la Cierva 3, 28006 Madrid, Spain

Received 10 October 1997; accepted 17 February 1998

ABSTRACT: Morphological properties of polymer electrolytes based on blends of polyethylene oxide and a perfluorinated polyphosphazene solvated with $LiCF_3SO_3$ with and without the addition of dispersed γ-$LiAlO_2$ are reported. The effect exerted on the morphology of the complex electrolytes by the addition of a plasticizer-like propylene carbonate has also been studied. Results indicate the incorporation of γ-$LiAlO_2$ leads to changes on the morphology of the complex electrolyte, as verified by X-ray diffraction analysis. The major effect observed by plasticizer addition was a decrease on the crystallinity of the system together with a displacement of the T_g towards lower temperatures. © 1998 John Wiley & Sons, Inc. J Appl Polym Sci 69: 2435–2440, 1998

Key words: polyelectrolytes; lithium; PEO; composites; morphology

INTRODUCTION

Polymer electrolytes have been extensively investigated after the discovery that reasonable high ionic conductivity can be achieved in solid state polymers complexed with lithium salts.[1] Various studies have focused on understanding the fundamental processes underlying ionic conductivity, ionic association, and morphology in polymer–salt complexes,[2–6] due to potential applications such as solid-state batteries, fuel cells, electrochromic displays, and chemical sensors. One of the more widely studied polymer–salt complex is poly(ethylene oxide) (PEO) complexed with lithium trifluoromethanesulfonate (triflate) $LiCF_3SO_3$. The phase diagram show that at least three phases coexist: (a) crystalline PEO below the melting point at around 70°C; (b) the crystalline compound $[PEO]_x$ $LiCF_3SO_3$, which melts around 155–185°C; and (c) an amorphous phase containing PEO and the $[PEO]_x$ $LiCF_3SO_3$ system,[7] this latter phase being responsible for ionic conduction while the former two inhibit ionic conductivity.[1]

It has been known that in the process of lithium salt dissolution in the polymer, in addition to the formation of a new crystalline phase due to the polymer–salt complex, there is an increase in the glass transition temperature,[8,9] both of which constrain the diffusion of the lithium ions through the membrane. To solve this problem, new polymer electrolytes based on blends, copolymers, etc., have been developed.[10,11] Other problems deal with the poor mechanical properties and dimensional stability of some synthesized solid polymer electrolytes, together with the existence of an electrochemical stability window associated with the polymer electrolyte, out of which irreversible redox processes takes place on the polyelectrolyte that enables its use in lithium batteries with a large choice of redox couples as cathode materials. Mechanical properties can be improved by addition of a finely dispersed solid filler to the polymer electrolyte, which provides a rigid matrix without significantly affecting polymer conductiv-

Correspondence to: E. Morales.

Contract grant sponsor: Nacional de Investigación Científica y Desarrollo Tecnológico; contract grant number: Mat95 0203.

Journal of Applied Polymer Science, Vol. 69, 2435–2440 (1998)

 CCC 0021-8995/98/122435-06

Table I Denomination and Sample Composition

	Composition				
Sample	PEO	PPz	γ-$LiAlO_2$	PC	O/Li^+ Molar Ratio
PEO	100	0	0	0	0
PEO/PPz	80	20	0	0	0
ELE3	80	20	0	0	8
ELE3P	80	20	0	80	8
ELE3Al10	80	20	10	0	8
ELE3Al20	80	20	20	0	8
ELE3PAl10	80	20	10	80	8
ELE3PAl20	80	20	20	80	8

ity.[12–15] In this article we have carried a comparative study of the morphological properties of $[PEO/PPz]_8LiCF_3SO_3$ electrolytes with and without γ-$LiAlO_2$ to assay the effects of the ceramic powder addition on the crystalline morphology of the polymer electrolyte. In a second stage, a parallel study was made by incorporating a plasticizer, propylene carbonate, to the composite polymer electrolyte.

EXPERIMENTAL

All the preparation procedures were carried out in an argon-filled dry box with a water content $\leq$1 ppm. PEO (Aldrich, M_w = 5,000,000) was dried under vacuum at 60°C for 24 h and stored inside the dry box. Poly(octofluoropentoxy-trifluoro-ethoxy phosphazene) (PPz) was supplied by Firestone under the trade name PNF200. This polymer was purified by dissolving in acetone and precipitated with a high excess of distilled water, then dried under vacuum at 100°C 24 h and stored inside the dry box. Propylene carbonate, PC (anhydrous, 99.7%) was an Aldrich product and was used as received. Lithium trifluoromethanesulfonate, $LiCF_3SO_3$ (Aldrich) was dried under vacuum at 120°C for 24 h. The ceramic filler γ-$LiAlO_2$ (Aldrich) was dried under vacuum at 140°C for 24 h. Polymer electrolytes were obtained by dissolving the appropriate amounts of polymers and salt in acetonitrile (Aldrich, no further purification), then casting over PTFE plates. Solid polymer electrolytes and blends were prepared by dissolving the appropriate amounts of polymers and lithium salt in acetonitrile, then casting over PTFE plates, and dried under vacuum until constant weight. For composite electrolyte preparation, γ-$LiAlO_2$ was added to this solution and finely dispersed in it by an ultrasonic stirrer. All solid polymer electrolytes contains an O : Li molar ratio of 8 : 1. Plasticized samples contains an 80 wt % of propylene carbonate. The amount of ceramic filler was 0, 10, and 20 wt %. Sample denomination and compositions are compiled in Table I.

Glass transition temperatures and thermograms were recorded in a Mettler TA4000 differential scanning calorimeter operated under nitrogen. Samples were loaded in hermetically sealed aluminum pans, heated to 220°C, and held there for 5 min to erase any previous thermal history, and then cooled to −120°C at a cooling rate of 20°C/min. The melting thermograms of the samples were obtained by heating up the samples to 220°C at a heating rate of 10°C/min. Thermograms in which two or more peaks overlapped were deconvoluted using a peak analysis software package (Peakfit from Jandel Scientific) using a five-parameter adjusting equation.

Infrared spectra were collected on a Nicolet 520 FTIR system at 2 cm^{-1} resolution. Sodium chloride plates were used as windows for the polymer complexes and lithium salt.

X-ray diffraction spectra of the samples were obtained using a Siemens D-500 diffractometer with a Ni-filtered CuK X-ray beam excited at 40 kV. Solid polyelectrolyte films were obtained by casting from acetonitrile solutions directly onto glass sample holders, then sealed with Mylar cellotape to avoid any contact with air. Spectra were recorded at $10 \leq 2\theta \leq 40$ for PEO and $10 \leq 2\theta \leq 50$ for solid polyelectrolytes with goniometer speed 0.5 deg(21)/min.

Table II Glass Transition Temperatures and Melting Parameters Measured on the First and Second Melting Cycles for PEO and the Different Electrolytes

		First Heating								Second Heating			
Sample	T_g[a] (°C)	T_{11} (°C)	ΔH_{11} (J/g)	T_{12} (°C)	ΔH_{12} (J/g)	T_{13} (°C)	ΔH_{13} (J/g)	T_{14} (°C)	ΔH_{14} (J/g)	T_{21} (°C)	ΔH_{21} (J/g)	T_{22} (°C)	ΔH_{22} (J/g)
PEO	−51.7	75.8	174.9	—	—	—	—	—	—	68.4	132.5	—	—
PEO/PPz	−52.1	67.7	157.8	—	—	—	—	—	—	67.6	152.9	—	—
ELE3	—	—	—	—	—	149.3	10.0	172.9	17.2	67.3	23.8	159.5	27.0
ELE3P	−56.5[b]	33.2	3.9	48.3	9.0	118.0	4.6	184.7	3.8	48.2	14.7	114.1	6.7
ELE3Al10	−43.4	—	—	74.1	35.0	146.4	17.2	181.3	9.8	69.8	27.9	152.6	26.1
ELE3Al20	−16.3	—	—	71.2	32.3	—	—	182.7	18.8	67.9	25.2	151.3	19.3
ELE3PAl10	−85.2	—	—	59.1	18.8	—	—	—	—	51.7	16.2	130.1	9.7
ELE3PAl20	−80.6	—	—	56.5	15.3	153.9	9.5	—	—	51.1	13.8	128.1	7.9

[a] Measured on the "as-cast" melting thermogram.
[b] Measured on the second melting thermogram.

RESULTS AND DISCUSSION

Thermal Behavior

Glass transition temperatures values, measured on the midpoint on the thermal flow jump, for "as-cast" samples are compiled in Table II, except for ELE3P sample where it was not possible to obtain an accurate measurement, given the value obtained in the second heating thermogram as an approximate value. Results indicate that the glass transition of the unplasticized complexes are shifted towards higher temperatures, as expected due to the lower degree of chain movements as a result of oxygen coordination.[16] Plasticized samples show lower values of T_g. The composite complexes show, as expected, higher T_g values related to the level of ceramic filler added, resulting from the restraint of chain movements promoted by the solid particles. Plasticized composite complexes show very low T_g values (down to −80°C), even much lower than the glass transition temperature of the plasticized polyelectrolyte free of γ-$LiAlO_2$.

Figure 1 show the melting thermograms of "as-cast" ELE3, ELE3P, and the four composite polymer electrolytes tested. Melting parameters obtained in the first and second heating scans are also compiled in Table II. All samples, except the composite ELE3PA110, present two melting regions; one located around 70–75°C for the unplasticized samples, and 56–59°C for the plasticized ones, corresponding to the melting of uncomplexed PEO, and a second region at higher temperatures, showing one or more peaks, associated with the crystalline polymer–salt complex. It has to be noticed that samples that show two endothermic peaks on the first heating cycle show only one transition in this region on the second heating cycle (Fig. 2), this attributable to a reorganization through equilibrium to give a single peak, which is a unique polymer–salt crystalline structure with a stochiometric polymer–salt composition. The melting temperatures of plasticized samples are lower than that of plasticizer-free samples.

Relating to the enthalpy values, it is clear that polymer electrolytes are less crystalline than pure PEO. Comparing data from the second heating cycle, where all samples have the same thermal history, it can be observed that the incorporation of the ceramic filler γ-$LiAlO_2$ has practically no

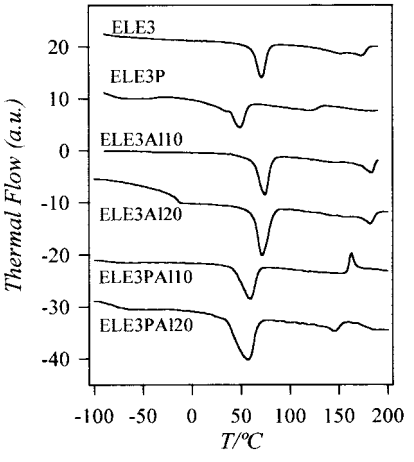

Figure 1 DSC melting thermograms of composite polymer electrolytes.

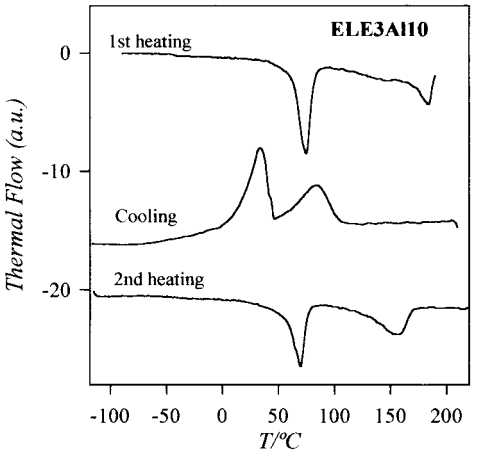

Figure 2 Cooling and first and second melting thermograms obtained for ELE310Al polymer electrolyte.

effect on the enthalpy of the peak associated with the free nonassociated PEO, while the value corresponding to the polymer–salt complex decreases as γ-$LiAlO_2$ concentration increases. Plasticized samples present enthalpy values lower than the unplasticized ones, having the ceramic filled polyelectrolytes again showing values slightly higher than in the absence of γ-$LiAlO_2$, again decreasing as γ-$LiAlO_2$ concentration increases.

FTIR Spectroscopy

It has been known that the degree of solvation and the influence of the anion properties on the morphology of the polymer significantly affect the spectral feature of polymer electrolytes. The vibrational spectra of PEO has been extensively studied,[17–22] and the detailed assignments of Yoshihara et al.[17] are generally accepted. Absorptions assigned to the methylene group (CH_2) unit occur in three different regions. These include the strong band near 2900 cm^{-1} (symmetric and antisymmetric stretching modes), and the less intense, but similarly shaped, bands at about 1460 cm^{-1} (asymmetric CH_2 bending) and 843 cm^{-1} (CH_2 rocking).

The strong band at 1108 cm^{-1} (asymmetric C—O—C stretching) is strongly affected by cation complexation, but is in a region rich in absorptions due to the anion. It has been described[23] that this band shifts to lower wavenumbers when salt is added. In our case, however, the band was found to remain at the same wavenumber (1108 cm^{-1}) (Fig. 3) for ELE3 electrolyte, while a new band appears at 1090 cm^{-1}. The incorporation of the ceramic filler leads to a split of this band in three bands, the maximum of them located at 1110 cm^{-1}, together with two new bands located at 1105 and 1113 cm^{-1}, plus a shoulder band at

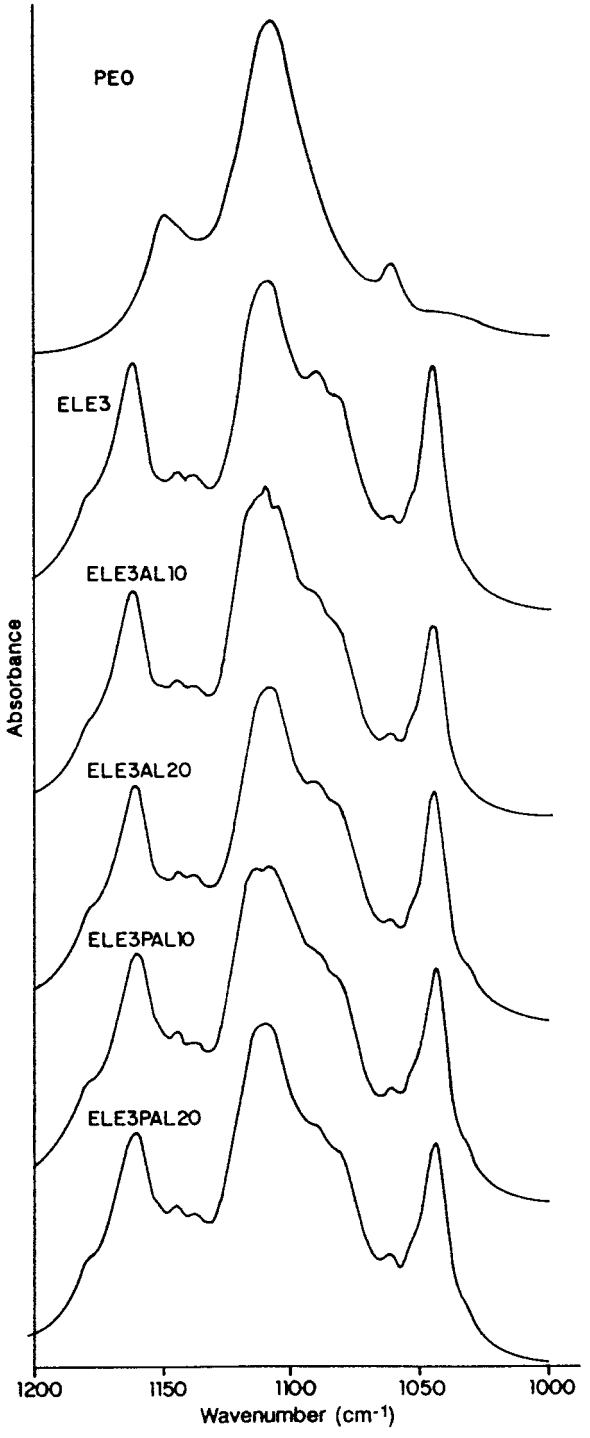

Figure 3 Infrared spectra of PEO, PPz, ELE3, and the composite polymer electrolytes studied in the spectral region between 1000 and 1200 cm^{-1}.

1091 cm^{-1}. When the level of γ-$LiAlO_2$ increase up to 20% a single band appears, centered at 1108 cm^{-1} plus the shoulder at 1091 cm^{-1}. Similarly for plasticized samples, the band appears split for the sample with lower γ-$LiAlO_2$ concentration (1108, 1113 cm^{-1}), while a single band at 1110 cm^{-1} is recorded for the 20% plasticized sample spectra.

The C—H stretching band centered at about 2900 cm^{-1} is also quite sensitive to the extent of salt complexation, as are the bending and rocking modes around 1460 and 843 cm^{-1} respectively.

Figure 4 present the FTIR spectra in the region 2650 to 3100 cm^{-1} for PEO, PPz, together with that for complexes ELE3, ELE310Al, and ELE320A1. Uncomplexed PEO show a band with a maximum centered at 2891 cm^{-1} and three shoulder peaks located, respectively, at 2947, 2877, and 2863 cm^{-1}. When PEO was complexed with lithium salt, it can be observed that spectra are similar, appearing a band at 2888 cm^{-1} in all cases plus a more defined shoulder peak located around 2935 cm^{-1}.

Relating to the C—H rocking mode absorption (not shown in the graph), the absorption band that appears at the 843 cm^{-1} for PEO is split into three bands for ELE3 polymer electrolyte (834, 843, and 860 cm^{-1}) remains the same situation for all the composite polymer complexes.

X-ray Spectroscopy

The crystal structure of PEO was first proposed by Tadokoro et al.[24] and consist of a 7/2 helix, that is seven ethylene oxide repeat units with two twist in the helix. Figure 5 show the X-ray diffractograms of PEO, the ceramic filler γ-$LiAlO_2$, and the polymer electrolytes ELE3, ELE310Al, and ALE3P10Al. Examination of these diffractograms confirms that the polymer electrolyte ELE3 show a complex crystalline structure, which clearly differs from that of the original PEO crystals. The addition of γ-$LiAlO_2$ lead to diffractograms that contain the diffractions of polymer electrolyte ELE3, those of γ-$LiAlO_2$ and new bands that did not appear on any of the other compounds, thus indicating that the morphology of the electrolytes has been change as a result of filler addition. The addition of the propylene carbonate plasticizer has no effect on crystalline morphology, and only an increase on the amorphous halo extent was observed.

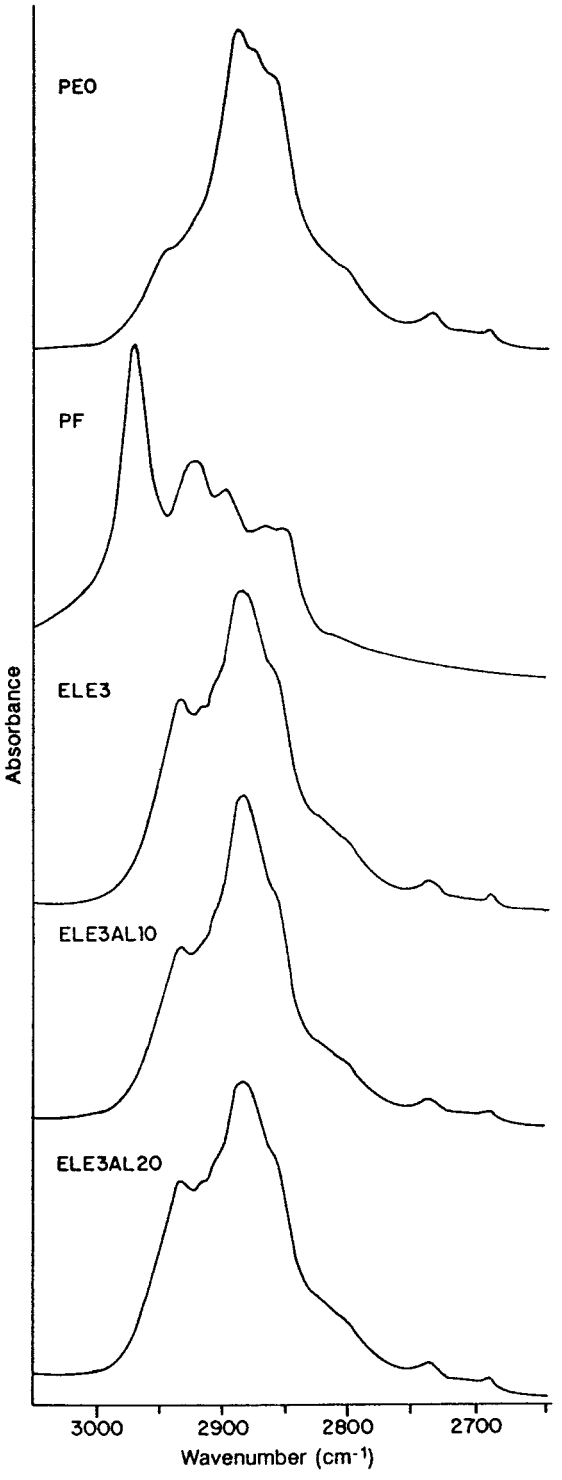

Figure 4 Infrared spectra of PEO, PPz, and the polymer electrolytes ELE3, ELE3A110, and ELE3A120 in the spectral region between 2650 and 3050 cm^{-1}.

CONCLUSIONS

As a general conclusion of the study we can stated that the solvation of polyethylene oxide with

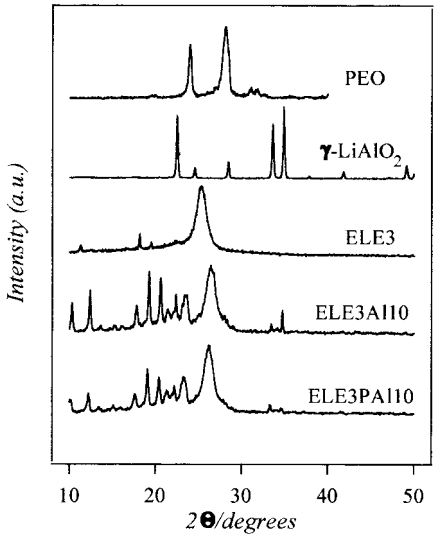

Figure 5 X-ray diffractograms of PEO, the ceramic filler, and ELE3, ELE310A1, and ELE320A1 polymer electrolytes.

$LiCF_3SO_3$ leads to a drastic change on the morphology of the system, resulting of the formation of a crystalline polymer–salt complex. The incorporation to the system of γ-$LiAlO_2$ at low concentrations has a little effect on the morphology, while an increase of the concentration of ceramic filler leads to changes in the morphology of the polymer–salt complex. At the same time, there seems to be no great interaction between the ceramic and the uncomplexed polymer. The incorporation of propylene carbonate decreases the crystallinity of the system, but the morphology of the crystalline regions remain unaltered.

REFERENCES

1. M. B. Armand, J. M. Chabagno, and M. J. Duclot, in *Fast Ion Transport in Solids,* P. Vashita, J. N. Mundy, and G. Shenoy, Eds., North Holland, New York, 1979.
2. S. Schantz, L. M. Torell, and J. R. Stevens, *J. Chem. Phys.,* **94,** 6862 (1991).
3. R. D. Armstrong and M. D. Clarke, *Solid State Ionics,* **11,** 305 (1984).
4. J. P. Le Nest and A. Gandini, in *Proceedings of the 2nd International Symposium on Polymer Electrolytes,* B. Srosati, Ed., Elsevier, Amsterdam, 1990.
5. R. Frech, J. Manning, and B. Black, *Polymer,* **30,** 1785 (1989).
6. J. Manning, R. Frech, and E. Hwang, *Polymer,* **31,** 2245 (1990).
7. R. Frech and S. Chintiapalli, *Solid State Ionics,* **85,** 61 (1996).
8. W. Wiekzorek, Z. Florjancyk, and J. R. Stevens, *Electrochim. Acta,* **40,** 2251 (1995).
9. J. L. Acosta and E. Morales, *Solid State Ionics,* **85,** 85 (1996).
10. K. Nagaoka, H. Naruse, I. Shinohara, and M. Watanabe, *J. Polym. Sci., Polym. Lett.,* **22,** 659 (1984).
11. X. Andrieu, J. F. Fauvarque, A. Goux, T. Hamaide, R. M'hamdi, and T. Vicedo, *Electrochim. Acta,* **40,** 2295 (1995).
12. J. E. Weston and B. C. H. Steele, *Solid State Ionics,* **7,** 75 (1982).
13. F. Croce, F. Bonino, S. Panero, and B. Scrosati, *Philos. Mag.,* **59,** 161 (1989).
14. B. Scrosati and F. Croce, *Pol. Adv. Technol.,* **4,** 198 (1993).
15. M. C. Borghini, M. Mastragostino, S. Passerini, and B. Scrosati, *J. Electrochem. Soc.,* **142,** 2118 (1995).
16. M. C. Wintersgill, J. J. Fontanella, S. G. Grennbaun, and K. J. Adamic, *Br. Polym. J.,* **20,** 195 (1988).
17. T. Yoshihara, H. Tadokoro, and S. Murahashi, *J. Chem. Phys.,* **41,** 2902 (1964).
18. W. H. T. Davidson, *J. Chem. Soc.,* 3270 (1995).
19. T. Miyazawa, K. Fukushima, and Y. Ideguchi, *J. Chem. Phys.,* **37,** 2764 (1962).
20. A. Miyake, *J. Am. Chem. Soc.,* **82,** 3040 (1960).
21. M. Shimomura, Y. Tanabe, Y. Watanabe, and M. Kobayashi, *Polymer,* **31,** 1411 (1990).
22. V. M. Da Costa, T. G. Fiske, and L. B. Coleman, *J. Chem. Phys.,* **101,** 2746 (1994).
23. S. J. Wen, T. J. Richardson, D. I. Ganthous, K. A. Striebel, P. N. Ross, and E. J. Cairns, *J. Electroanal. Chem.,* **408,** 113 (1996).
24. H. Tadokoro, Y. Chatani, T. Yoshihara, S. Tahara, and S. Murahashi, *Makromol. Chem.,* **73,** 109 (1964).